



Get Clarity On Generics

Cost-Effective CT & MRI Contrast Agents

**FRESENIUS
KABI**

WATCH VIDEO

AJNR

**Nontuberculous Mycobacterial Infection of the
Head and Neck in Immunocompetent Children:
CT and MR Findings**

Caroline D. Robson, Rohan Hazra, Patrick D. Barnes, Richard L.
Robertson, Dwight Jones and Robert N. Husson

This information is current as
of August 9, 2025.

AJNR Am J Neuroradiol 1999, 20 (10) 1829-1835
<http://www.ajnr.org/content/20/10/1829>

Nontuberculous Mycobacterial Infection of the Head and Neck in Immunocompetent Children: CT and MR Findings

Caroline D. Robson, Rohan Hazra, Patrick D. Barnes, Richard L. Robertson, Dwight Jones, and Robert N. Husson

BACKGROUND AND PURPOSE: Infections caused by nontuberculous mycobacteria (NTM) commonly manifest as cervicofacial adenitis in otherwise healthy children. The aim of this study was to characterize the imaging findings of NTM infection of the head and neck in immunocompetent children.

METHODS: The medical records and imaging examinations (CT in 10, MR in two) were reviewed in 12 immunocompetent children with NTM infection of the head and neck.

RESULTS: The usual presentation ($n = 9$) was of an enlarging, non-tender mass with violaceous skin discoloration, unresponsive to conventional antibiotics. The duration of symptoms was 6 days to 5 months. Imaging revealed asymmetric adenopathy with contiguous low-density ring-enhancing masses in all patients. There was cutaneous extension in 10 patients. Inflammatory stranding of the subcutaneous fat was minimal ($n = 9$) or absent ($n = 2$) in 11 patients. The masses involved the submandibular space ($n = 3$), the parotid space ($n = 2$), the cheek ($n = 1$), the anterior triangle of the neck ($n = 2$), the submandibular and parotid spaces ($n = 2$), the parotid space and neck ($n = 1$), and the neck and retropharyngeal space ($n = 1$). Surgical management included incision and drainage only ($n = 2$), incision and drainage with curettage ($n = 2$), excisional biopsy after incision and drainage ($n = 1$), excisional biopsy only ($n = 5$), superficial parotidectomy only ($n = 1$), and superficial parotidectomy with contralateral excisional biopsy ($n = 1$). All patients improved in response to surgery and long-term antimycobacterial antibiotics.

CONCLUSION: NTM infection of the head and neck has a characteristic clinical presentation and imaging appearance. Recognition of this disease is important; appropriate treatment is excision and, in selected cases, antimycobacterial therapy.

During the past few decades infections caused by nontuberculous mycobacteria (NTM) have been recognized with increasing frequency. NTM infections commonly manifest as cervicofacial adenitis in immunocompetent children under 5 years old. The traditional treatment of choice for cervicofacial NTM adenitis has been excisional biopsy because incision and drainage may lead to recurrence or sinus tract formation (1–4). The diagnosis of NTM

adenitis, however, is often delayed. NTM infection may be considered only after persistence or progression of adenitis despite antibiotic and surgical therapy for presumed staphylococcal or streptococcal infection, or after excision with histopathologic and microbiological examination. The recognition of characteristic imaging features distinguishing NTM from suppurative bacterial adenitis would allow earlier institution of appropriate therapy. The purpose of our study was to describe the imaging findings of NTM infections of the head and neck in immunocompetent children. The clinical manifestations, differential diagnosis, and treatment are also discussed.

Methods

Patients

A list of all children who had NTM adenitis involving the head and neck during a 5-year period was obtained using a database from the Division of Infectious Diseases. In this database, children were assigned a diagnosis of NTM adenitis if

Received April 8, 1999; accepted July 8.

From the Department of Radiology (C.D.R., P.D.B., R.L.R.), the Division of Infectious Diseases, (R.H., R.N.H.), and the Department of Otolaryngology (D.J.), Children's Hospital and Harvard Medical School, Boston, MA.

Presented at the Annual Meeting of the American Society of Head and Neck Radiology, Phoenix, AZ, April 1998 and at the 36th Annual Meeting of the American Society of Neuroradiology, Philadelphia, PA, May 1998.

Address reprint requests to Caroline D. Robson, MBChB, Dept. of Radiology, Children's Hospital, 300 Longwood Ave., Boston, MA 02115.

© American Society of Neuroradiology

they met one of the following criteria: 1) culture of a lymph node specimen was positive for mycobacteria; 2) characteristic findings were found on histologic examination of a lymph node specimen (large well-formed granulomas composed of epithelioid histiocytes, multinucleated giant cells, mononuclear inflammatory cells, and extensive areas of acellular, often caseous, necrosis) with or without staining positive for acid-fast bacilli; or 3) patient was referred to the Division of Infectious Diseases because of persistent cervical, submandibular, or preauricular adenopathy without warmth, tenderness, or fever (5). The medical records and imaging examinations of those patients with NTM infection who were known to be immunocompetent and who had undergone either CT or MR imaging were reviewed. Only patients who were culture-positive for NTM ($n = 9$) or had necrotizing granulomatous inflammation with positive stains for acid fast bacilli and negative skin testing with purified protein derivative ($n = 3$) were selected. This group of 12 children included eight girls and four boys ranging in age from 9 months to 4 years old at the time of initial presentation. The medical records were reviewed for history, physical examination, operative findings, laboratory results, pathologic findings, treatment, and subsequent follow-up (Table). A recent review emphasizing the clinical presentation and therapy of lymphadenitis owing to NTM included five of the 12 patients (5).

CT Protocol

Using either a GE 9800 or Advantage CT scanner (General Electric Medical Systems, Milwaukee, WI), ten children were imaged with CT of the head and neck. Patients were scanned with 5-mm contiguous axial images from the skull base to the thoracic inlet during a bolus intravenous injection of 2 cc/kg Ioversol 68% (w/v) (Optiray 320, Mallinckrodt Medical Inc., St. Louis, MO). Images were obtained using 120 kV, 170–200 mA, a 1–2 sec scan time, a 15–25-cm field of view (FOV), and a 512×512 matrix.

MR Protocol

Two patients underwent MR imaging of the head and neck on a 1.5-T system (General Electric Medical Systems, Milwaukee, WI) using a volume neck coil. The imaging protocol consisted of axial and coronal fast spin-echo inversion recovery images (4000/32/2 [TR/TE/excitations]; TI, 150 ms; 5-mm slice thickness; 2-mm interslice gap; 24×18 -cm FOV; 256×192 matrix) or fast spin-echo T2-weighted images with fat suppression (3200/78/1 [TR/TE/excitations]; 5-mm slice thickness; 1-mm interslice gap; 24-cm FOV; 256×192 matrix) and axial T1-weighted conventional spin-echo images (500/16/2 [TR/TE/excitations]; 5-mm slice thickness; 2-mm interslice gap; 24×18 -cm FOV; 256×160 matrix). After the intravenous administration of 0.1 mmol/kg of gadopentetate dimeglumine (Magnevist, Berlex Laboratories, Wayne, NJ), axial T1-weighted spin-echo images with fat suppression were obtained (700/16/2 [TR/TE/excitations]; 5-mm slice thickness; 2-mm interslice gap; 24×18 -cm FOV; 256×160 matrix). One patient who underwent CT of the neck also underwent MR imaging of the brain with line-scan diffusion-weighted imaging (1520/62.5/1 [TR/TE/excitations]; 7-mm nominal slice thickness; 0-mm interslice gap; 20×15 -cm FOV; 128×128 matrix; b maximum = 750 s/mm^2) for evaluation of cerebral infarction. This patient also underwent cerebral angiography.

Image Review and Analysis

Two pediatric neuroradiologists reviewed the imaging findings. The studies were evaluated for the number, location, and size of neck masses, density or intensity characteristics, enhancement pattern, presence or absence of skin thickening, stranding of subcutaneous fat, presence or absence of necrosis, presence or absence of calcification, and bone involvement.

Results

Clinical History

All 12 patients (Table) presented with a gradually enlarging neck mass ($n = 8$) or masses ($n = 4$). The duration of symptoms ranged from 1 week to 4 months (median, 4.5 weeks). Violaceous skin discoloration over the mass was present in 10 patients. Symptoms of low-grade fever and slight tenderness were noted in three patients. These patients had only 1- to 3-weeks' duration of symptoms. One of these patients developed a right hemiplegia prior to admission. Systemic symptoms were absent in the remaining nine patients. In all patients, the masses were firm and non-tender or minimally tender to palpation. None of the children had evidence of immunodeficiency. Skin testing with purified protein derivative was weakly positive in five patients, negative in five, equivocal in one, and not performed in one.

Imaging

The cervicofacial masses were single in eight children and multiple in four. The locations of the masses are given in the Table. The masses occurred most often in the submandibular space ($n = 5$), and within the parotid space ($n = 5$). Other sites included the cheek, the retropharyngeal space, and the anterior or posterior triangle of the neck (Table). The maximum lymph node diameter was approximately 2 centimeters except in one child who had an aggregate of lymph nodes measuring 4×3 cm (case 4). The masses consisted of heterogeneously enhancing adenopathy with contiguous low density (CT, Fig 1) or high intensity (T2-weighted MR, Fig 2) necrotic ring-enhancing lesions in all patients. The ring-enhancing lesions were subcutaneous with cutaneous extension in 10 patients, and measured 1.0–2.5 cm in diameter in all patients. Stranding of the adjacent subcutaneous fat was typically minimal ($n = 9$) or absent ($n = 2$). In one patient (case 5) the mass did not extend to the skin, and stranding of the subcutaneous fat was moderate. Multiple low-density ring-enhancing lymph nodes were noted in two patients (cases 8 and 10, Fig 3). Stippled calcification was also present in one (case 10, Fig 4). Bone involvement was not detected in any patient.

One patient, who had a hemiplegia (case 11), had a mass in the left parotid region (Fig 5A) and was found to have acute cerebral infarction involving the left basal ganglia on MR images (Fig 5B–C). No leptomeningeal enhancement was seen. Cerebral angiography showed mild, smooth narrowing of the left supraclinoid internal carotid artery.

Surgical, Histopathologic, and Culture Results

Incision and drainage only ($n = 2$), or incision and drainage with curettage ($n = 2$) was performed in four patients in whom the diagnosis of NTM

Summary of clinical and imaging data for 12 children

Case	Age/Sex	Duration of Mass	Location of Mass Other Symptoms	Necrosis	Stranding of Fat	Cutaneous Extension	Ca ⁺⁺	PPD	Therapy	Histology	Culture
1	2y 6mo/F	2 mo	Submandibular	+	Minimal	+	-	+	I & D & curettage Clarithromycin Ethambutol	ND	<i>M. intracellulare</i>
2	2y/M	6 wk	Cheek	+	Minimal	+	-	+/-	Excisional biopsy Clarithromycin Rifampin	Necrotizing granulomatous inflammation AFB	<i>M. avium</i>
3	4y/F	1 wk	Submandibular Parotid Low grade fever	+	Minimal	+	-	ND	I & D Excisional biopsy Clarithromycin Ethambutol Rifampin Rifabutin	Necrotizing granulomatous inflammation AFB	NTM, not MAI
4	1y/M	1 mo	Neck	+	Minimal	+	-	-	Excisional biopsy Clarithromycin Ethambutol Rifabutin	Necrotizing granulomatous inflammation AFB	<i>M. avium</i>
5	2y/M	2 wk	Submandibular	+	Moderate	-	-	-	I & D Clarithromycin Ethambutol	Necrotizing granulomatous inflammation AFB	ND
6	2y/F	3 wk	Submandibular Low grade fever	+	Minimal	+	-	+	I & D Clarithromycin Rifampin	Necrotizing granulomatous inflammation AFB	<i>M. avium</i>
7	4y/F	2 mo	Parotid Submandibular	+	Absent	+	-	-	Excisional biopsy Azithromycin Rifampin Clarithromycin Ethambutol Rifabutin	Necrotizing granulomatous inflammation AFB	Negative
8	2y 6mo/F	4 wk	Posterior neck Retropharyngeal	+	Absent	+	-	-	Excisional biopsy Clarithromycin Rifampin	Necrotizing granulomatous inflammation AFB	<i>M. avium</i>
9	2y 3mo/M	5 wk	Parotid	+	Minimal	-	-	+	Superficial parotidectomy Clarithromycin Rifampin	Necrotizing granulomatous inflammation AFB	<i>M. avium</i>

Continued

Case	Age/Sex	Duration of Mass	Location of Mass Other Symptoms	Necrosis	Stranding of Fat	Cutaneous Extension	Ca ⁺⁺	PPD	Therapy	Histology	Culture
10	2y 9mo/F	4 mo	Parotid Neck	+	Minimal	+	+	-	Superficial parotidectomy Excisional biopsy Clarithromycin Rifampin Ethambutol	Necrotizing granulomatous inflammation AFB	Negative
11	9mo/F	1 wk	Parotid Low grade fever Hemiplegia	+	Minimal	+	-	+	Excisional biopsy Clarithromycin Rifampin Ethambutol	Necrotizing granulomatous inflammation AFB	<i>M. avium</i>
12	3yr/F	4 mo	Neck	+	Minimal	+	-	+	I & D & curettage Clarithromycin Rifampin	Necrotizing granulomatous inflammation AFB	<i>M. avium</i>

Note.—y = year; mo = month; wk = week; F = female; M = male; ND = not done; I & D = incision and drainage; AFB = acid-fast bacilli.

adenitis was not suspected or because excision was thought to pose a significant risk. Incision and drainage followed by excisional biopsy was performed in one patient, and excisional biopsy alone was performed in five patients. Two patients underwent superficial parotidectomy, including excision of contralateral lymph nodes in one patient. The incised or excised masses contained purulent material in all patients and appeared grossly caseous in two patients. Necrotizing granulomatous inflammation and acid-fast bacilli were present in all patients from whom histopathologic samples were obtained and analyzed (n = 11). Nontuberculous mycobacterial species were cultured in nine patients, including *Mycobacterium avium* complex in eight patients. Culture was negative (n = 2) or not performed (n = 1) in three patients in whom acid-fast bacilli were identified by histopathologic analysis. These three patients were purified protein derivative negative (Table).

All patients received long-term antimycobacterial therapy with double or triple drug regimens. These included various combinations of clarithromycin, ethambutol, rifabutin, rifampin, clofazimine, and azithromycin. Gradual improvement occurred in all patients over a 3- to 18-month period. Two patients, however, developed new masses after 4 months of follow-up.

Discussion

A wide variety of diseases are caused by NTM, including disseminated infections in immunocompromised patients, pulmonary infections predominantly in adults with underlying lung disease, and lymphadenitis in healthy children (5, 6). Unlike bacterial adenitis, NTM infection often is unresponsive to conventional antibiotics or incision and drainage. Therefore, recognition of the clinical and radiologic features that distinguish NTM from other head and neck infections is important for instituting appropriate therapy.

Clinical Presentation

NTM species are ubiquitous in soil and water, and are carried by domestic and wild animals, including birds (7). It is generally accepted that humans acquire these organisms from environmental sources (7, 8). Cervical lymphadenitis may result from ingestion of NTM. Persistent cervicofacial lymphadenitis is the most common manifestation of NTM infection in children and usually occurs in otherwise healthy children under 5 years old (peak age, 2 to 4 years old) (3, 7). *Mycobacterium avium* or *Mycobacterium intracellulare* accounts for most cases of NTM lymphadenitis. Disseminated disease is usually restricted to immunocompromised individuals.

The clinical manifestations of NTM adenitis are considered characteristic (1, 3, 9–13). The disease usually presents as a slowly enlarging and unilateral submandibular or preauricular mass of nodes.

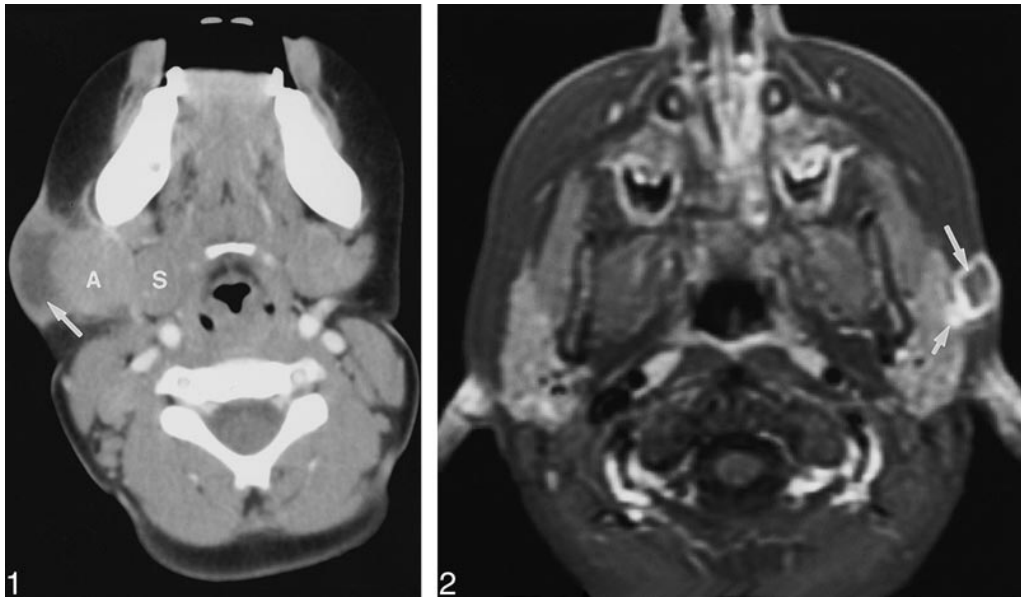


FIG 1. Case 1: Girl, 2 years six months old, with nontender right submandibular mass. Axial contrast-enhanced CT scan shows medial displacement of right submandibular gland (S) by right submandibular adenopathy (A). Suppurative granulomatous material represented by low-density ring-enhancing subcutaneous mass (arrow) extending from adenopathy to skin. Minimal stranding of adjacent subcutaneous fat is present.

FIG 2. Case 7: Four-year-old girl with masses in left preauricular and submandibular regions. Axial contrast-enhanced fat-suppressed T1-weighted, 700/16/2 (TR/TE/excitations), conventional spin-echo MR image, demonstrates low signal intensity lesion (arrow) with ring enhancement, which corresponded to purulent material at surgery. Mass extends from superficial surface of left intraparotid lymph node (short arrow) to skin. No stranding of the adjacent subcutaneous fat is present.

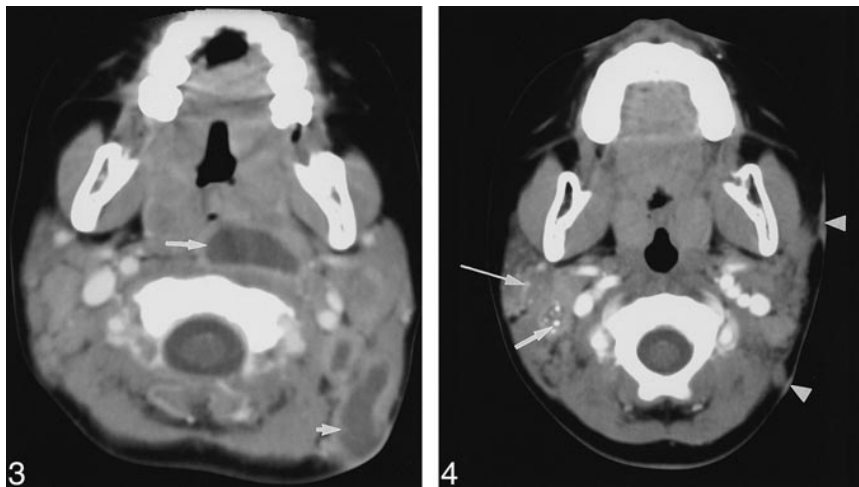


FIG 3. Case 8: Girl, two years six months old, with 4-week history of enlarging left posterior triangle neck mass and deviation of oropharynx to right. Axial contrast-enhanced CT scan shows low-density ring-enhancing spinal accessory adenopathy (short arrow) with extension to skin. Enlarged low-density ring-enhancing left retropharyngeal adenopathy (long arrow) causing distortion and narrowing of oropharynx is present.

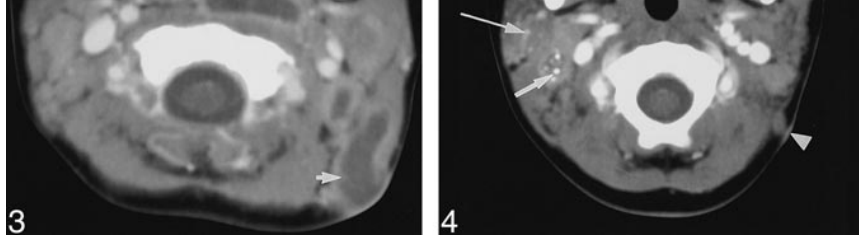


FIG 4. Case 10: Girl, two years nine months old, with right parotid and right cervical adenopathy. Axial contrast-enhanced CT scan demonstrates punctate calcification within low-attenuation ring-enhancing lymph node (arrow), posterolateral to right internal jugular vein. Calcification within right intraparotid adenopathy (long arrow) is visible. Two foci of left-sided skin thickening (arrowheads) adjacent to adenopathy are present.

Fever or other systemic signs of infection usually are absent (5). Extranodal extension may involve the contiguous subcutaneous fat, an adjacent salivary gland, or the skin. In the absence of effective therapy, the mass typically progresses to liquefaction. There is violaceous discoloration of the overlying skin followed by spontaneous drainage through the skin (5). The affected region is typically non-tender, or minimally tender, and signs of acute inflammation are lacking.

A delay in diagnosis is common because most cases are presumed to represent suppurative bacterial adenitis. As a result, standard antibiotic therapy is instituted but fails. Culture, isolation, and

identification of the organisms may take an additional 2 to 6 weeks. The duration of symptoms is typically weeks to months before a definitive diagnosis is made.

To our knowledge, the association of NTM adenitis and stroke in immunocompetent children has not been reported. Culture of *Mycobacterium avium* complex from an intracranial aneurysm, however, has been reported in a patient with the acquired immunodeficiency syndrome (14). Although immunocompetent children with NTM adenitis typically lack systemic symptoms, the occurrence of a stroke in one of our patients suggests that occasionally the disease process may be more generalized. In this patient, the

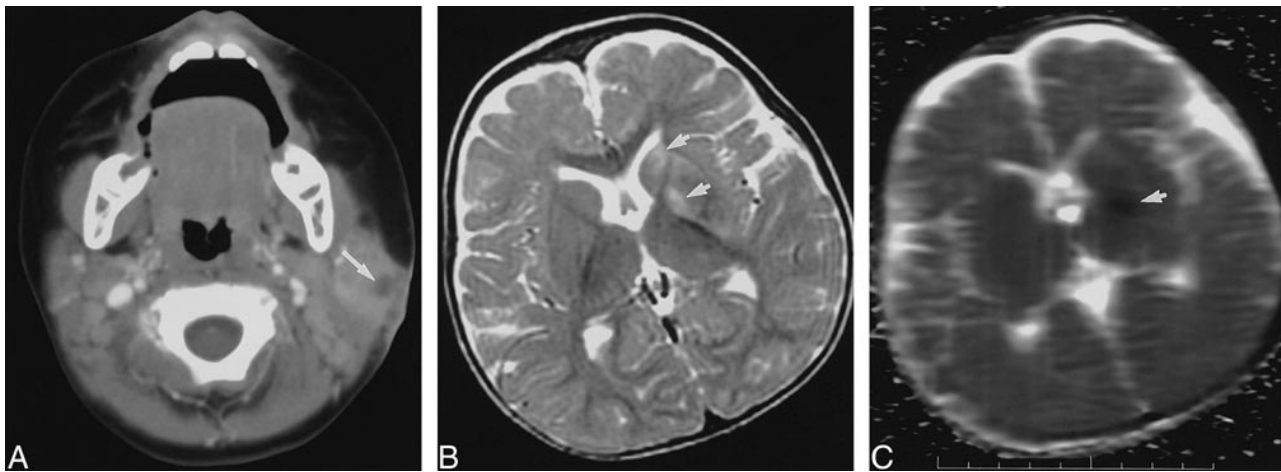


FIG 5. Case 11: Nine-month-old girl with left parotid mass and right hemiplegia.

A, Axial contrast-enhanced CT scan shows focal low density (arrow) within left parotid gland with thickening of adjacent subcutaneous fat and skin.

B, Axial T2-weighted (3200/78/1) fast spin-echo MR image demonstrates high signal intensity involving left corpus striatum (arrows).

C, Axial apparent diffusion coefficient map from line-scan diffusion image (1520/62.5/1; b maximum = 750 s/mm²) shows low signal intensity (arrow) indicating decreased diffusion associated with acute or subacute infarction. Although immunocompetent children with NTM adenitis typically lack systemic symptoms, occurrence of cerebral infarction, possibly owing to vasculitis, in this patient suggests that occasionally the disease process may be more generalized.

presence of supraclavicular internal carotid artery narrowing may have indicated a vasculitis.

Imaging

Little has been written about the imaging features of NTM cervical adenitis. In our patients both CT and MR imaging displayed characteristic imaging features and adequately defined the extent of disease. In our series, adenopathy most commonly arose near the angle of the mandible or within the parotid space. Involvement of the retropharyngeal space was unusual and simulated a retropharyngeal abscess (Fig 3). Contrast-enhanced axial CT scans most commonly demonstrated asymmetric cervical lymphadenopathy and contiguous low-density, necrotic, ring-enhancing masses involving the subcutaneous fat and skin. Unlike conventional bacterial abscesses in our patients with NTM adenitis, inflammatory stranding of the subcutaneous fat was typically minimal or absent. The clinical history and CT findings suggested a bacterial abscess in only one patient (case 5), whereas CT scans demonstrated moderate stranding of the subcutaneous fat and a lack of cutaneous involvement. Punctate calcification of cervical lymph nodes was uncommon.

Differential Diagnosis

The differential diagnosis of the imaging appearance of NTM infection includes bacterial adenitis, tuberculous adenitis, cat-scratch disease, fungal infection, tularemia, brucellosis, infected branchial cleft cyst, infected lymphatic malformation, treated lymphoma, and other necrotic neoplasms (3, 8). The treatment of choice for NTM adenitis is excision of the affected lymph nodes.

Therefore, it is important to distinguish this condition from bacterial adenitis that is usually treated with incision and drainage. In contrast to NTM, common forms of bacterial adenitis and cat-scratch disease tend to produce painful unilateral or bilateral enhancing lymph nodes, which may appear as low attenuation on CT scans if necrotic (15). Extensive stranding of the adjacent subcutaneous fat is a common associated finding.

Tuberculosis usually produces painless bilateral posterior triangle and internal jugular adenitis. Unlike our patients with NTM, tuberculous adenitis typically is seen in a child who is systemically ill and also has pulmonary disease. The presence of a conglomerate nodal mass on CT scans with central lucency and thick rims of enhancement and minimally effaced fascial planes has been reported to be suggestive of tuberculous adenitis, especially if the patient has a strongly reactive tuberculosis skin test (16). Calcification of lymph nodes is considered also to be highly suggestive of tuberculous adenitis (17), but was present in one of our patients with NTM (case 10). A retropharyngeal mass caused by mycobacteria is usually related to cervical tuberculous osteomyelitis but may result occasionally from NTM infection (18). In cases of suspected NTM infection, tuberculosis may be excluded by history of exposure, absence of pulmonary disease, and by the absence of systemic manifestations of disease. Purified protein-derivative tests are usually strongly positive in tuberculous adenitis but are reportedly positive in only 55% of patients with *Mycobacterium avium* complex with a slightly higher reactivity in patients with other nontuberculous mycobacteria (19). When positive, purified protein-derivative skin testing in patients with NTM adenitis is typically only weakly reactive (20).

The laboratory diagnosis of mycobacterial infection involves the use of routine histopathologic stains, acid-fast smears, and mycobacterial cultures. Necrotizing granulomatous inflammation is found with both tuberculosis and NTM infections, as well as other granulomatous diseases. Stains for acid-fast bacilli are reportedly positive in only 20% to 50% of patients with positive skin tests and histopathologic results consistent with NTM infection (20). Even when staining shows bacilli, these organisms may fail to grow in culture (21). Culture recovery is reported to occur approximately 50–80% of most series of patients (1, 3, 11, 12). The most commonly cultured species in NTM adenitis is *Mycobacterium avium* complex (21–23). In patients who are culture negative, NTM infection is suggested by the appropriate clinical history, physical examination, and pathologic findings in the absence of a history of exposure to tuberculosis or cats.

Management

Surgical excision is currently the treatment of choice for NTM adenitis (3, 9, 11). Fine-needle aspiration biopsy has been recommended as a rapid and safe means of obtaining material for testing and confirmation of the diagnosis prior to excision of the mass (11). Curettage has been recommended by some authors for any lesion adjacent to facial nerve branches or for lesions with extensive skin necrosis that would otherwise require flap coverage (11). Treatment with incisional biopsy or a drainage procedure usually is not adequate and may lead to recurrence or the formation of a draining sinus tract or fistula (3, 20).

NTM infections are difficult to treat medically and respond poorly to traditional antituberculous therapy. Medical treatment has been recommended for patients who refuse surgery or for NTM infection that persists after surgery (24, 25). Medical therapy with a regimen that includes clarithromycin has shown promise in the treatment of immunocompetent patients (5).

Conclusion

NTM infection should be considered in an afebrile child younger than 5 years who presents with painless unilateral submandibular or preauricular adenitis. Additional supportive evidence includes a negative family history of tuberculosis, a negative or mildly reactive purified protein-derivative skin test, and a lack of systemic symptoms. Our experience suggests that NTM adenitis has a typical imaging appearance. It is characterized by asymmetric cervical lymphadenopathy, one or more contiguous low-density ring-enhancing masses involving the subcutaneous fat and skin, and negligible inflammatory stranding of the subcutaneous fat. The recognition of the characteristic imaging features of NTM infection should allow earlier diagnosis and institution of appropriate therapy.

References

1. Akhtar J, Howatson AG, Raine PA. **Atypical mycobacterial infection in childhood: a "surgical disease".** *J R Coll Surg Edinb* 1997;42:110–111
2. Kanlikama M, Gokalp A. **Management of mycobacterial cervical lymphadenitis.** *World J Surg* 1997;21:516–519
3. Stewart MG, Starke JR, Coker NJ. **Nontuberculous mycobacterial infections of the head and neck.** *Arch Otolaryngol Head Neck Surg* 1994;120:873–876
4. Taha AM, Davidson PT, Bailey WC. **Surgical treatment of atypical mycobacterial lymphadenitis in children.** *Pediatr Infect Dis* 1985;4:664–667
5. Hazra R, Robson CD, Perez-Atayde AR, Husson R. **Lymphadenitis due to nontuberculous mycobacteria in children: presentation and response to therapy.** *Clin Infect Dis* 1999;28:123–129
6. Inderlied CB, Kemper CA, Bermudez LE. **The mycobacterium avium complex.** *Clin Microbiol Rev* 1993;6:266–310
7. Chadwick EG, Rosenfeld EA. **Nontuberculous mycobacterium species.** In: Long SS, Pickering LK and Prober CG, eds. *Pediatric Infectious Diseases*. Vol 1. 1st ed. New York: Churchill Livingstone; 1997:904–910
8. Starke JR. **Nontuberculous mycobacterial infections in children.** *Adv Pediatr Infect Dis* 1992;7:123–159
9. Castro DJ, Hoover L, Zuckerbraun L. **Cervical mycobacterial lymphadenitis. Medical vs surgical management.** *Arch Otolaryngol* 1985;111:816–819
10. Joshi W, Davidson PM, Jones PG, Campbell PE, Robertson DM. **Non-tuberculous mycobacterial lymphadenitis in children.** *Eur J Pediatr* 1989;148:751–754
11. Tunkel DE, Romaneschi KB. **Surgical treatment of cervicofacial nontuberculous mycobacterial adenitis in children.** *Laryngoscope* 1995;105:1024–1028
12. Thompson JN, Watanabe MJ, Greene GR, Morozumi PA, Kohut RI. **Atypical mycobacterial cervical adenitis: clinical presentation.** *Laryngoscope* 1980;90:287–294
13. Suskind DL, Handler SD, Tom LW, Potsic WP, Wetmore RF. **Nontuberculous mycobacterial cervical adenitis.** *Clin Pediatr (Phila)* 1997;36:403–409
14. Destian S, Tung H, Gray R, Hinton DR, Day J, Fukushima T. **Giant infectious intracavernous carotid artery aneurysm presenting as intractable epistaxis.** *Surg Neurol* 1994;41:472–476
15. Dong PR, Seeger LL, Yao L, Panosian CB, Johnson BL, Jr, Eckardt JJ. **Uncomplicated cat-scratch disease: findings at CT, MR imaging, and radiography.** *Radiology* 1995;195:837–839
16. Reede DL, Bergeron RT. **Cervical tuberculous adenitis: CT manifestations.** *Radiology* 1985;154:701–704
17. Vazquez E, Enriquez G, Castellote A, et al. **US, CT, and MR imaging of neck lesions in children.** *Radiographics* 1995;15:105–122
18. Rice DH, Dimcheff DG, Benz R, Tsang AY. **Retropharyngeal abscess caused by atypical mycobacterium.** *Arch Otolaryngol* 1977;103:681–684
19. O'Brien RJ, Geiter LJ, Snider DE, Jr. **The epidemiology of nontuberculous mycobacterial diseases in the United States. Results from a national survey.** *Am Rev Respir Dis* 1987;135:1007–1014
20. Stanley RB, Fernandez JA, Peppard SB. **Cervicofacial mycobacterial infections presenting as major salivary gland disease.** *Laryngoscope* 1983;93:1271–1275
21. Wolinsky E. **Mycobacterial lymphadenitis in children: a prospective study of 105 nontuberculous cases with long-term follow-up.** *Clin Infect Dis* 1995;20:954–963
22. Grange JM, Yates MD, Pozniak A. **Bacteriologically confirmed non-tuberculous mycobacterial lymphadenitis in south east England: a recent increase in the number of cases.** *Arch Dis Child* 1995;72:516–517
23. Kuth G, Lamprecht J, Haase G. **Cervical lymphadenitis due to mycobacteria other than tuberculosis—an emerging problem in children?** *ORL J Otorhinolaryngol Relat Spec* 1995;57:36–38
24. Mandell F, Wright PF. **Treatment of atypical mycobacterial cervical adenitis with rifampin.** *Pediatrics* 1975;55:39–43
25. Margileth AM. **Management of nontuberculous (atypical) mycobacterial infections in children and adolescents.** *Pediatr Infect Dis* 1985;4:119–121